Kinetics of Charge Accumulation and Decay on Silicone Rubber/SiO$_2$ Nanocomposite Surface

Yong Liu[†], Zhong-Lei Li* and Bo-Xue Du*

Abstract – The accumulation and decay of surface charge on silicone rubber (SiR)/SiO$_2$ nanocomposites under a unipolar corona discharge field was investigated. The effect of the weight ratio of SiO$_2$ nanoparticles from 0.1 to 0.7 wt.% was studied. Attenuated total reflection infrared spectra of the SiR/SiO$_2$ nanocomposites indicated that the SiO$_2$ nanoparticles chemically and physically interacted with the SiR matrix. This facilitated the SiR chains in restricting the injection of surface charge into the bulk nanocomposite. SiR composites containing SiO$_2$ nanoparticles (especially that containing 0.1 wt.% SiO$_2$) exhibited significantly reduced surface discharge. This approach may have application in outdoor SiR electrical insulators.

Keywords: Silicone rubber/SiO$_2$ Nanocomposites, Surface charge, Charge accumulation, Charge decaying

1. Introduction

The surface charging processes and characteristics of composite dielectrics have received much interest. This is particularly relevant to analyzing surface discharge in an electric field, for insulated electrical and electronic devices [1-3]. Silicone rubber (SiR) composites are typical outdoor electrical insulating materials [4, 5]. Under high voltage (HV), electrons emitted from HV conductors, and positive and negative ions remain together. These can be injected into SiR insulating surfaces to form surface charge. This is a major cause of surface degradation and surface discharge [6-8]. Accumulated surface charge should be avoided or efficiently relaxed, to protect SiR materials against insulation failure.

The dynamic behavior of surface charge in insulating polymers has been recently investigated. Gubanski et al. reported spatial and temporal distributions of surface charge on ethylene propylene diene monomer rubber and SiR, with varying voltages and pulse numbers. They also investigated the mechanism of surface potential decay in high-temperature-vulcanized SiR in relation to air and bulk properties [9-11]. Li et al. reported the charge transport of epoxy resin/glass composition (FR4), poly-tetrafluoroethylene and polyimide. Their focus was on evaluating spacecraft charging, and predicting surface and internal electrostatic discharging [12]. Laurent et al. reported that charge transport and trapping in low-density polyethylene was influenced by surface states. An

exponential distribution of traps with a maximum trap depth was used to explain this result [13]. Du et al. reported the effect of nanofiller concentration on the surface charge accumulation and decay of epoxy/TiO$_2$, epoxy/BN and polyimide/Al$_2$O$_3$ nanocomposites. Charge dynamics were found to depend on localized surface states, the characteristics of which were altered by the nanoparticles [14-16].

Understanding the effect of SiO$_2$ nanoparticles on the surface charge kinetics of SiR/SiO$_2$ composites remains a challenge. In the current study, the accumulation and decay of surface charge in SiO$_2$ nanoparticle-loaded SiR composites was investigated. The effect of SiO$_2$ nanoparticle different weight ratios was investigated.

2. Experimental Arrangement

Neat room-temperature-vulcanized SiR (Shenzhen Anpin Silicone Material Co., Ltd.) without solid fillers was employed. Spherical SiO$_2$ nanoparticles (Nanjing Haitai Nanomaterials Co., Ltd) of average diameter of ~20 nm were surface treated to avoid agglomeration. The nanoparticles were dried in a desiccator for >24 h, before being dispersed in SiR. Samples with dimensions of 35×35×2.5 mm were prepared by incorporating 0.1, 0.3, 0.5, and 0.7 wt.% SiO$_2$ nanoparticles into SiR matrices. Undoped samples were investigated for comparison. Fig. 1 shows a scanning electron microscopy (SEM) image of the nanoparticle distribution. Most nanoparticles were well-dispersed in the SiR matrix.

A schematic of the surface charge measurement apparatus is shown in Fig. 2. Surface charge was measured using a pair of needle-plated electrodes, coupled with a grid electrode at room temperature. The needle electrode

†   Corresponding Author: Key Laboratory of Smart Grid of Ministry of Education (Tianjin University), School of Electrical Engineering and Automation, Tianjin University, China. (tjuliuyong@tju.edu.cn)
*   Key Laboratory of Smart Grid of Ministry of Education (Tianjin University), School of Electrical Engineering and Automation, Tianjin University, China.
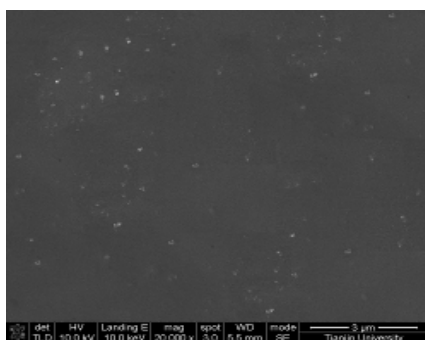
Fig. 1. SEM image of SiR/SiO$_2$ nanocomposite containing 0.1 wt.% SiO$_2$
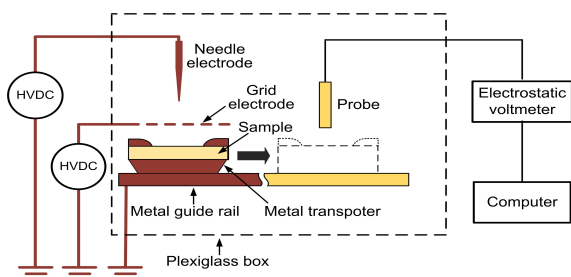

Fig. 2. Schematic of the apparatus used to measure surface charge.

had a diameter of 1 mm and tip radius of ~13 μm, and was connected to a +DC HV source. The needle tip was positioned 5 mm above the 35×35×0.4 mm grid electrode, the latter which was located 5 mm above the sample surface. The sample was placed on a metal transporter, which could move in one dimension along a grounded metal and epoxy guide rail. 6 kV was applied between the needle and the ground electrodes, and 4 kV was applied to the grid electrode. Corona charging tests were performed at room temperature and relative humidity of ~40 %. The charging time was 10 min.

After the corona charging test, the sample was quickly transferred to the underside of a non-contacting probe, to determine the surface potential. The Kelvin-type probe (Trek 6000B-5C) coupled with electrostatic voltmeter (Trek 347-3HCE) provided a measurement accuracy of ±3 V and spatial resolution of 3 mm. The probe-to-surface distance was 3 mm. The distances between the probe and electrodes were sufficiently large to avoid any influence of electric field distribution on the surface potential measurement. Surface potential decay curves were recorded by a computer.

3. Results and Discussion

3.1 Surface charge accumulation of SiR/SiO$_2$ nano-composite

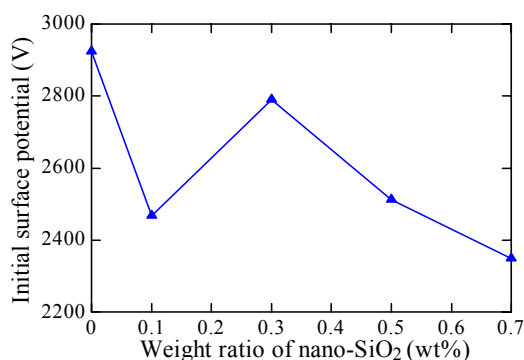Fig. 3 shows the dependence of initial surface potential

Fig. 3. Relationship between initial surface charge and SiO$_2$ nanoparticle weight ratio.

on the SiO$_2$ nanoparticle weight ratio. The initial surface potential was decreased by the presence of the nanoparticles. Thus, the SiO$_2$ nanoparticles suppressed surface charge accumulation in SiR. There was a significant interaction between the SiO$_2$ nanoparticles and SiR matrix, in which the SiR chains were chemically and/or physically bound to the nanoparticle surface. Charge accumulation largely arose from intrinsic defects within the molecular structure, so charge produced by the electric field was captured in the composite. The nanoparticles had a reducing effect on defects, which restrained charge injection to the bulk.
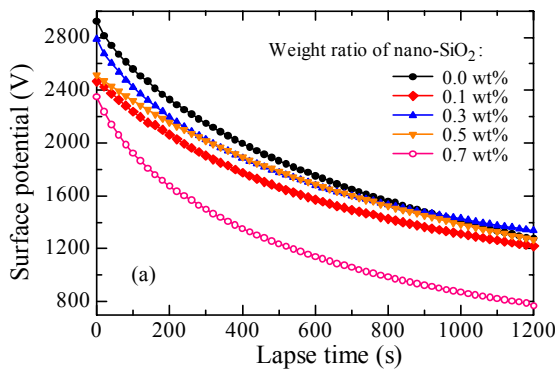
Fig. 3 shows a peak in initial surface potential at 0.3 wt.% SiO$_2$ nanoparticle loading, for the investigated SiR/SiO$_2$ nanocomposites. The potential at 0.1 wt.% was lower, and the potential decreased with increasing weight ratio from 0.3 to 0.7 wt.%. It was thought that charge was injected into the bulk through the specimen surface. With increasing weight ratio, more nanoparticles were bound to SiR chains through van der Waals forces, which could easily be destroyed by the outside electric field. The higher surface energy of nanoparticles caused injected charge to be electrostatically captured around the nanoparticles. This resulted in homogeneous charge layers, which restricted further charge injection. This accounted for the decreasing charge accumulation from 0.3 to 0.7 wt.%.

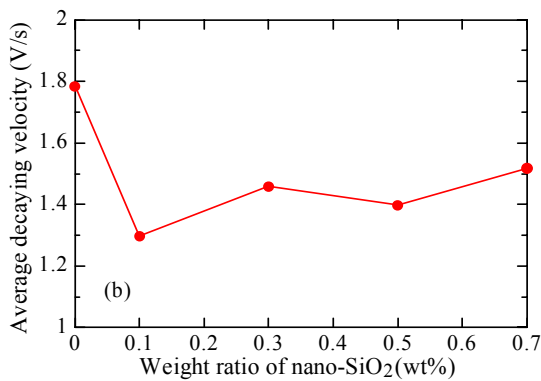### 3.2 Decaying characteristics of surface charge of SiR/SiO$_2$ nanocomposite

Fig. 4(a) shows the decay of surface charge with SiO$_2$ nanoparticle weight ratio. Surface charge initially rapidly decayed, and then slowly eased off with increasing lapse time. This indicated that injected charge induced a high electric potential. Accumulated charge was released from the composite, and then passed across the surface and/or through the bulk into the ground electrode.

The average decay velocity during the decay time was calculated from Eq. (1):

$$V_{decaying} = \frac{U_0 - U_t}{\Delta t} \tag{1}$$

(a) Decay of surface charge with increasing lapse time

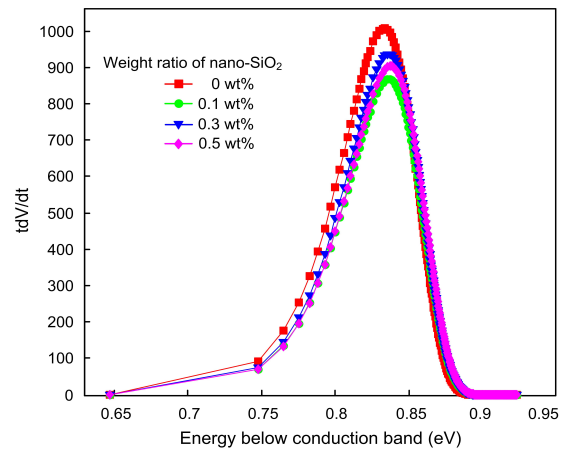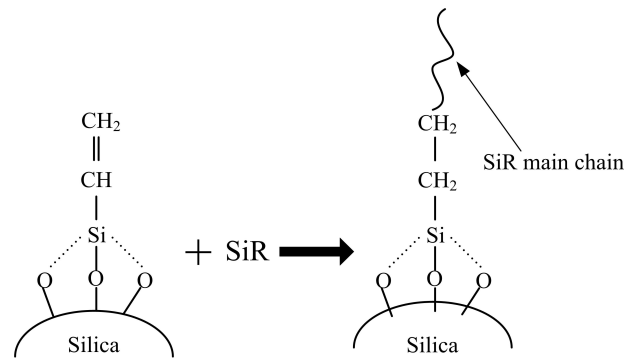(b) Average decay velocity of surface charge with increasing weight ratio

Fig. 4. Decay of surface charge with SiO$_2$ nanoparticle weight ratio

where $V_{Decaying}$ is the average decay velocity (V/s), and U_t is the surface potential at time t.

The relationship between average decay rate and weight ratio is shown in Fig. 4(b). The rate of decay in potential of the SiR/SiO$_2$ nanocomposites was slower than that of SiR. The lowest average decay velocity of surface potential occurred at 0.1 wt.% weight ratio. The decay velocity was largely constant from 0.3 to 1.0 wt.% SiO$_2$ nanoparticle content. This influence was considered to result from interaction zones formed by the nanoparticles. The increasing weight ratio may have led to overlapping interaction zones around nanoparticles, which were more reactive than those at lower mass fraction.

Fig. 5 shows the trap distributions of samples containing different SiO$_2$ nanoparticle weight ratios. Charge transport is typically associated with carrier trapping and de-trapping. The energy of traps is related to the lapse time by the demarcation energy, E_m, which indicates the border between unoccupied and occupied traps. With increasing time, E_m moves away from the conduction band, and the relationship between the lapse time and energy gap is defined as:

$$E_c - E_m = kT \ln(vt) \qquad (2)$$

Fig. 5. Trap distributions of SiR/SiO$_2$ nanocomposites with different SiO$_2$ nanoparticle weight ratios

Fig. 6. Schematic of the interaction between SiO$_2$ nanoparticles and SiR matrix

$$t \frac{dV(t)}{dt} \infty N(E_m(t)) \frac{dE_m}{dt} = N(E_m(t))kT \frac{N_t}{N_c} \tau_0 \qquad (3)$$

where E_c is the conduction band energy level, v is the attempt to escape frequency, tdv/dt is proportional to the trap energy density $N(E_m)$ at energy level $E_m(t)$, N_t and N_c are the trap and conduction state densities, respectively, and τ_0 is the carrier lifetime of conduction states.

3.3 Effects of Nano-SiO$_2$ particles on trap depth of nanocomposite

Fig. 5 shows that the trap depth in the SiR/SiO$_2$ nanocomposites was deeper than that in SiR. The shallow traps represented low energy levels, which could not obstruct the mobility of trapped charge. Thus, charge easily moved out from shallow traps. The well-dispersed nanoparticles in the matrix restrained charge transport in bulk SiR, and influenced the decay velocity of surface charge, as shown in Fig. 4. With increasing nanoparticle weight ratio, the overlap of interaction zones surrounding nanoparticles increased, and became more reactive than those at lower mass fraction. When many interaction zones overlapped, many conductive paths formed through the

overlap of the transition region in the bulk, thus reducing charge trapping. The minimum trap depth was at ~0.834 eV for neat SiR, and the average decay velocity was ~1.8 V/s, as shown in Fig. 4(b).

Fig. 6 shows a schematic of the interaction between SiO_2 nanoparticles and SiR matrix. Chemical species generated by association with nanoparticles can significantly influence charge accumulation and transport in nanocomposites. Fig. 6 shows that the SiR/SiO_2 interface contained electronic states associated with oxygen. The electronic structure and arrangement of SiR matrix and nanoparticles suggested that charge injection was restrained, by capture in the bulk composite. The nanoparticles increased the trap energy level, as shown in Fig. 5. Charge de-trapping could occur by thermally-activated electrons hopping from occupied oxygen sites to nearest-neighbor unoccupied oxygen sites. This lowered the delay velocity, compared with that of SiR. Increasing the SiO_2 nanoparticle weight ratio from 0.1 to 0.7 wt.% increased the delay velocity, as shown in Fig. 4. This was associated with overlapping interaction zones of the nanoparticles. The resulting overlapping layers were more reactive than those at lower weight ratio [17]. Many conductive paths formed through the overlap of the transition region in the bulk nanocomposite. These also reduced charge accumulation, and accelerated the de-trapping of surface charge.

4. Conclusion

In summary, the addition of SiO_2 nanoparticles of up to 0.7 wt.% improved the accumulation and decay of surface charge in SiR/SiO_2 nanocomposites, compared with SiR. The addition of 0.1 wt.% SiO_2 resulted in the lowest surface charge. The SiO_2 nanoparticles restricted surface charge from accumulating in the SiR composites, and resulted in a low surface charge after decay. This approach has application in the surface flashover of outdoor SiR electrical insulators.

Acknowledgements

References

[1] Seiffe J., Hofmann M., Rentsch J. and Preu R., "Charge Carrier Trapping at Passivated Silicon Surfaces", *J. Appl. Phys.*, vol. 109, no. 6, pp. 4505-4512, 2011.

[2] Son J. Y., Kyhm K. and Cho J. H., "Surface Charge Retention and Enhanced Polarization Effect on Ferroelectric Thin Films", *Appl. Phys. Lett.*, vol.89, no.9, pp. 2907-2909, 2006.

[3] Deng J., Kumada A., Hidaka K., Zhang G. and Mu H., "Residual Charge Density Distribution Measurement of Surface Leader With Feedback Electrostatic Probe", *Appl. Phys. Lett.*, vol. 100, no.19, pp. 2906-2909, 2012.

[4] Momen G. and Farzaneh M., "Survey of Micro/Nano Filler Use to Improve Silicone Rubber for Outdoor Insulators", *Rev. Adv. Mater. Sci.*, vol. 27, no. 1, pp. 1-13, 2011.

[5] Pradeep M. A., Vasudev N., Reddy P. V. and Khastgir D, "Effect of ATH Content on Electrical and Aging Properties of EVA And Silicone Rubber Blends for High Voltage Insulator Compound", *J. Appl. Polym. Sci.*, vol. 104, no. 6, pp. 3505-3516, 2007.

[6] Lagel B., Ayala M. D. and Schlaf R., "Kelvin Probe Force Microscopy on Corona Charged Oxidized Semiconductor Surfaces", *Appl. Phys. Lett.*, vol. 85, no. 20, pp. 4801-4803, 2004.

[7] Guaitella O., Marinov I. and Rousseau A., "Role of Charge Photodesorption in Self-Synchronized Breakdown of Surface Streamers in Air at Atmospheric Pressure", *Appl. Phys. Lett.*, vol. 98, no. 7, pp. 1502-1504, 2011.

[8] Li M., Li C. R., Zhan H. M., Xu J. B. and Wang X. X., "Effect of Surface Charge Trapping on Dielectric Barrier Discharge", *Appl. Phys. Lett.*, vol. 92, no. 3, pp. 1503-1505, 2008.

[9] Sjöstedt H., Gubanski S. M. and Serdyuk Y. V., "Charging Characteristics of EPDM and Silicone Rubbers Deduced from Surface Potential Measurements", *IEEE Trans. Dielectr. Electr. Insul.*, vol. 16, no. 3, pp. 696-703, 2009.

[10] Sjöstedt H., Montaño R., Serdyuk Y. and Gubanski S. M., "Charge Relaxation on Surfaces of Polymeric Insulating Materials for Outdoor Applications", *Mater. Sci.-Poland*, vol. 27, no. 4, pp. 1129-1137, 2009.

[11] Kumara S., Serdyuk Y. V. and Gubanski S. M., "Surface Charge Decay on Polymeric Materials under Different Neutralization Modes in Air", *IEEE Trans. Dielectr. Electr. Insul.*, vol. 18, no. 5, pp. 1779-1788, 2011.

[12] Min D. M., Cho M., Khan A. R. and Li S. T, "Charge Transport Properties of Dielectrics Revealed by Isothermal Surface Potential Decay", *IEEE Trans. Dielectr. Electr. Insul.*, vol. 19, no. 4, pp. 1465-1473, 2012.

[13] Du B. X. and Li J., "Electrified Droplet on Corona-Charged Surface of Silicone Rubber/SiO_2 Nanocomposite", *IEEE Trans. Dielectr. Electr. Insul.*, vol. 19, no. 6, pp. 2073-2080, 2012.

[14] Du B. X., Zhang J. W. and Gao Y., "Effects of TiO_2 Particles on Surface Charge of Epoxy Nanocomposites", *IEEE Trans. Dielectr. Electr. Insul.*, vol. 19,

no. 3, pp. 755-762, 2012.

[15] Du B. X., Li J. and Du W., "Surface Charge Accumulation and Decay on Direct Fluorinated Polyimide/Al$_2$O$_3$ Nanocomposites", *IEEE Trans. Dielectr. Electr. Insul.*, vol. 20, no. 5, pp. 1764-1771, 2013.

[16] Du B. X. and Xiao M., "Influence of Surface Charge on DC Flashover Characteristics of Epoxy/BN Nano-composites", *IEEE Trans. Dielectr. Electr. Insul.*, vol. 21, no. 2, pp. 529-536, 2014.

[17] Wintle H. J., "Surface Charge Decay in Insulators with Nonconstant Mobility and With Deep Trapping", *J. Appl. Phys.*, vol. 43, no. 7, pp. 2927-2930, 1972.

Yong Liu He received the M.E. and Ph.D. degrees in electrical engineering from Tianjin University, China, in 2006 and 2009, respectively. Since 2009, he has been a Lecturer, and then an Associate Professor at School of Electrical Engineering and Automation in Tianjin University, China. From 2014 to 2015, he was a Research Fellow with the NSERC / Hydro-Quebec / UQAC Industrial Chair on Atmospheric Icing of Power Network Equipment, Canada. His main research interests are ageing evaluation and performance monitoring of outdoor insulators under various atmospheric conditions.

Zhong-Lei Li He received the B.S. degree in electrical engineering from Tianjin University, China, in 2011. He is now pursuing the Ph.D. degree at School of Electrical Engineering and Automation in Tianjin University. His research interests include dielectric property improvements and space charge of polymer insulating materials.

Bo-Xue Du He received the M.E. degree in electrical engineering from Ibaraki University and the Ph.D. degree from Tokyo University of A&T. During 1996-2002, he was with Niigata College of Technology, Japan and was an Associate Professor. From 2000 to 2002, he was a Visiting Scientist at Niigata University, Japan. Since 2002 he has been a Professor at the Department of Electrical Engineering, School of Electrical Engineering and Automation, Tianjin University, China. His research interests are focused on dielectric failure mechanisms of polymer insulating materials, electrical insulation technology and partial discharge measurements. He is a member of IEEJ and senior member of CSEE, member at several WG in CIGRE and an Associate Editor of the IEEE Transactions on Dielectrics and Electrical Insulation.